Length of multi-year precipitation and primary production relationships vary regionally across grasslands in the central U.S.

Hudson, A.R.*; Peters, D.P.C.*
* USDA ARS SCINet Big Data Program, Beltsville, MD

Key words: Climate change; wavelet coherence

Abstract

Grasslands in the central United States span large temperature and aridity gradients and regionally differ in their drivers of water availability. These differences likely determine how drought event periodicity and duration can influence grassland growth, and are important to consider as global warming changes energy and water distribution across these systems. Here, we explored frequency patterns in annual grassland plant growth (aboveground net primary productivity (ANPP)) and precipitation (PPT) relationships for over 20 years at six long-term research sites spatially distributed across the central grassland region. We identified the periods (>1 year) these relationships are strongest- and when they occur- with wavelet coherence analyses. We found disturbance events such as severe drought lowered ANPP and preceded strong coherence at 2-4 year periods at two sites, potentially by increasing ANPP sensitivity to PPT. All sites showed strong coherence at 1-2 years periods, however this coherence was not consistent through time for two sites, where declines in ANPP did not correspond with PPT variability. In addition to strong coherence at 1-2 year periods, at southern desert and central tallgrass grasslands there was also strong coherence at 5-10 year periods over the entire record, indicating that long-term PPT and ANPP dynamics are important. Pacific ocean-atmosphere drivers of regional precipitation were found to influence coherence at all sites, and could potentially explain the long-term 5-10 year coherence at the sites mentioned above. Contextualizing ANPP-PPT relationships through time at sites with different drivers of precipitation requires understanding of site-dependent production dynamics and is key to forecasting grassland responses to climate change.

Introduction

Grasslands of the central U.S. (Fig. 1) span a wide swath of latitudes and climate, with warmer temperatures to the south and wetter conditions to the east promoting diverse grassland systems (Lauenroth and Burke 1995). Annual measures of plant production and community composition at central U.S. grassland sites have been linked to precipitation at multiple scales, including at multi-year, annual, seasonal, sub-seasonal and event characteristics (e.g. Chen et al. 2017, Petrie et al 2017, Collins et al. 2020, Peters et al. 2021, Hudson et al. 2022). However, few studies have examined how precipitation and plant production relationships can vary over time scales or across the region.

To move from site-level production dynamics to a regional context requires the integration of broad scale climate drivers (Peters et al. 2008) such as the El Niño Oscillation (ENSO) and Pacific Decadal Oscillation (PDO)- sea surface temperature anomalies in the Pacific Ocean that interact with atmospheric variability to influence climate over the land surface (Mantua et al. 1997, Rayner et al. 2003). These semi-periodic drivers can also influence the frequency of site-level precipitation, which may further interact with cycles in plant life cycles to produce periods of high or low coupling strength between precipitation and plant production.

Our objectives here were to leverage long-term research at central U.S. grasslands to evaluate site and regional variability in the (1) coherence between annual aboveground net primary production (ANPP) and precipitation (PPT) across periods and time, and (2) potential climatic drivers (ENSO and PDO) of ANPP and PPT coherence.

Methods

Study sites: The United States' long-term ecological research (LTER) network was established in 1980 with a directive of core tasks, one of which was observing and testing primary production response to, for example, climate (Hobbie et al. 2003). Six current or former LTER grassland sites are spatially distributed across the central grassland region of the U.S. (Fig. 1; grassland delineations modified from Olson et al. (2001)), and represent the south to north cooling and west to east wetting gradients of the region. Semiarid to arid warm mixed grasslands are in central (Sevilleta, SEV) and southern (Jornada Basin, JRN) New Mexico; semiarid cool shortgrass steppe grasslands are in Colorado (Shortgrass Steppe, SGS); tallgrass prairie grasslands are in Kansas (Konza Prairie, KNZ); and mesic, cool grasslands are in Minnesota (Cedar Creek Ecosystem Science Reserve, CDR) and Michigan (Kellogg Biological Station, KBS; Fig. 1). SGS was an LTER site until 2014, and has been included in previous syntheses examining production - precipitation relationships (Petrie et al. 2017).

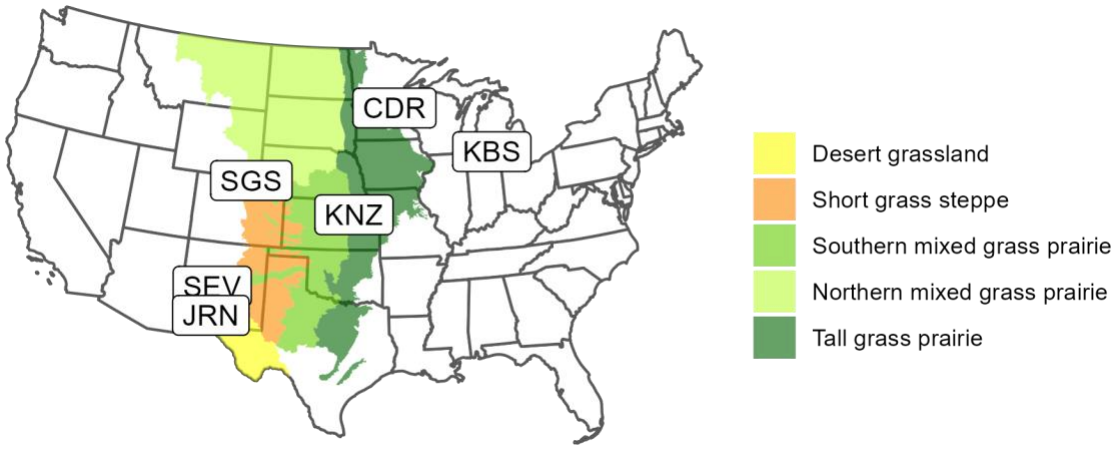

Figure 1. Map of long-term ecological research sites located across the central grasslands of the U.S. Grassland types along south to north and west to east gradients experience warmer and wetter climate conditions. JRN and SEV are desert grasslands, SGS is short grass steppe, and KNZ is tall grass prairie.

Data: At least 20 years of co-occurring PPT and ANPP site data were used in this study. PPT was summed across the water year (October - September; Sevilletta summed November to October). PPT sources and ANPP sources and methods for 5 sites are detailed in Hudson et al. (2022). For SGS, water year PPT was summed (Parton 2014) and ANPP was derived from annual biomass of annual and perennial grasses (both warm and cool season) averaged across ungrazed upland control plots (Lauenroth 2014) after identifying which species to extract from the LTER species list available at http://hdl.handle.net/10217/80451 (Shoop et al. 2022). 1991 ANPP was missing at SGS and was gap filled by averaging 1990 and 1992 values.

ENSO and PDO were represented with the Pacific Ocean sea surface temperature-derived Nino 3.4 index (https://psl.noaa.gov/gcos_wgsp/Timeseries/Data/nino34.long.data; Rayner et al. 2003) and PDO index (https://psl.noaa.gov/gcos_wgsp/Timeseries/Data/pdo.long.data; Mantua et al. 1997). Monthly values were averaged across the water year to match the temporal resolution of site precipitation data.

Analyses: We first identified and removed linear long-term trends in site ANPP and PPT, as well as climate teleconnections over the period of overlap with each site using the trend (Pohlert 2020) and pracma (Borchers 2021) package with R statistical software (v4.0.4; R Core Team 2021). There were significant increases in ANPP over time for JRN (Sen's slope = 3.08), SEV (Sen's slope = 2.38), and KBS (Sen's slope = 13.33), while there were slight but significant decreases in ANPP at SGS (Sen's slope = -0.17). KBS was the only site with a positive trend in annual PPT (Sen's slope = 7.90) which was mainly driven by winter and spring precipitation.

Obj. 1: We conducted bivariate wavelet coherence analyses between PPT and ANPP on periods of 1yr and greater at each site. This analysis evaluates the local correlation between two time series across the time-frequency domain to identify similar rhythmic components, and is useful for analyzing non-stationary signals of short duration (Hu et al. 2021). We used the biwavelet R package (Gouhier et al. 2021) where statistical significance levels were estimated with Monte Carlo methods with n = 1000 randomizations. Data on either end of the record indicate the "cone of influence," where edge effects become important and should not be interpreted. To simplify the wavelet plots, we also averaged the wavelet coherence at each period step outside the cone of influence. This approach allowed us to identify coherent periods across time and to contextualize all sites at once.

Obj. 2: We then determined how much influence PDO or ENSO may have on the coherence between PPT and ANPP by conducting partial wavelet coherence transforms (Gouhier et al. 2021, Hu et al. 2021). We report the percent area of significant coherence (PASC) between the resulting wavelet coherence maps (Hu et al. 2021; similar to methods in Zhou et al. 2022). To define PASC, we only considered where R^2 values were larger than 0.8 and outside the cone of influence as significant.

Results and Discussion

Obj. 1: Overall, the desert grassland sites JRN (Fig 2f) and SEV (Fig. 2e), tallgrass prairie site KNZ (Fig. 2d) and the Michigan site KBS (Fig. 2b) had the strongest coherence and highest PASC for periods longer than 1 year (JRN= 65%, SEV= 44%, KNZ = 53%, KBS =47%; Table 1). CDR (Fig. 2a) and SGS (Fig. 2c) show only 20% and 33% respectively, indicating that PPT is not as strong a driver of ANPP at these two sites for periods longer than 1 year (Table 1).

All sites had strong wavelet coherence between ANPP and PPT in the 1-2 year period band across their respective time domains (Fig. 2, Fig. 3). However, some sites experienced weaker coherence in the 1-2 year period for a subset of time, including 2005-2010 at CDR (Fig 2a) and 2006 to 2008 at SEV (Fig. 2e). In both cases, this was due to ANPP (gray lines in times series) showing little variability and negative trends over the time frame. Desert grassland sites (JRN and SEV) and tallgrass prairie (KNZ) had the strongest wavelet coherence between ANPP and PPT across periods larger than 2 years (red values in Fig. 2d, 2e, 2f). This result supports previous studies showing the importance of multi-year PPT periods to ANPP at the JRN (Peters et al. 2021), and indicates that modeling production response to precipitation at these sites in the south central U.S. would improve if multi-year periods were included.

Disturbance events such as severe drought may precede strong coherence between ANPP and precipitation at periods of 2-4 years. This result may be because drought reduced ANPP past a certain threshold such that ANPP was more responsive to precipitation following the disturbance (Collins et al., 2020). KNZ experienced a major drought in 1988-89 and the lowest ANPP on record, followed by strong 2-4 year coherence for another decade (Fig. 2d). Haddad et al. (2002) discuss how this drought may have contributed to 2-year oscillations in ANPP that lasted a decade. By 2000, the system returned to low coherence in the 2-4 year band (Fig. 2d). At SEV (Fig. 2e), in 2011 severe drought and reductions in ANPP preceded strong coherence across periods including the 2-4yr band.

All sites except for CDR had strong average wavelet coherence in the 7-yr period (Fig. 3). CDR and SEV had relative maximum average wavelet coherence in the 4-yr band (Fig. 3), while KNZ maximum coherence was at 9-yr and greater. JRN and KBS show similar patterns of maximum coherence at 2 and 7-yrs, and SGS also had maximum coherence at 7-yrs. CDR is most strongly coherent in the 4-yr period from 1985-2000 (Fig. 2a), which has some overlap with the periodicity of ENSO and PDO (Fig. 2g). SGS shows a similar coherence at 4-yr period but for a shorter time (1985-1995) and strongest in the cone of influence (Fig. 2c).

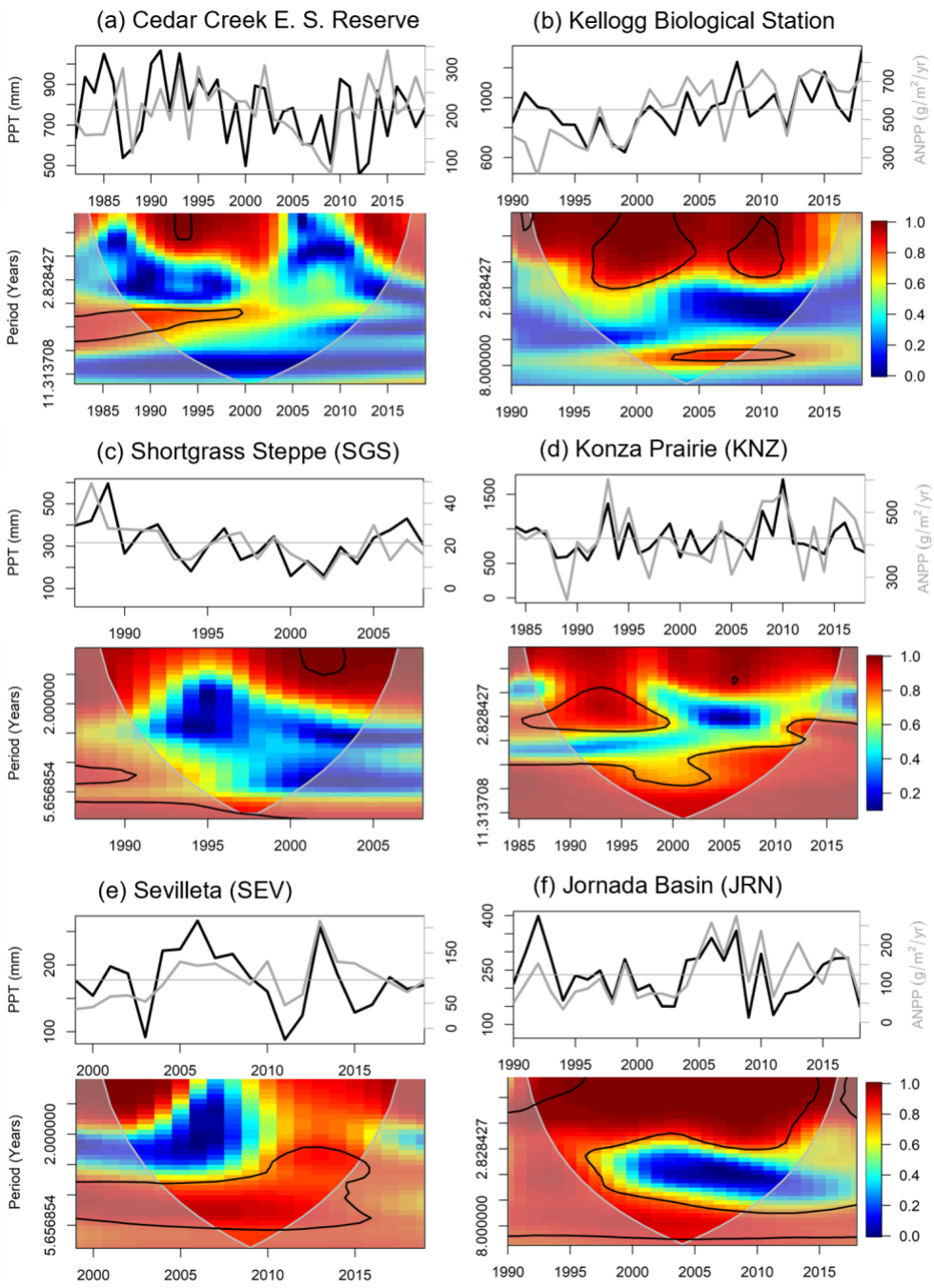

Figure 2. PPT and ANPP time series and wavelet coherence at the 6 LTER sites. PPT is on the left axis shown with black lines in mm per water year and ANPP is on the right axis with gray lines in g/m^2/year; the horizontal line on each time series plot shows the mean PPT and ANPP values over the period. The period length on the wavelet coherence plots' y-axis is measured in years. The color bar indicates the strength of coherence between PPT and ANPP, and ranges from 0 (low coherence, blue) to 1 (high coherence, red). Regions of significant coherence were contoured and determined based on Monte Carlo methods and chi-squared test for significance with alpha threshold of 0.95. Light gray shading shows the region influenced by edge effects (cone of influence) and should not be interpreted for those periods.

Table 1. Percent area of significant coherence (PASC) based on the wavelet coherence of ANPP and PPT (ANPP~PPT) and the partial wavelet coherence between ANPP and PPT after removing the effects of ENSO (ANPP~PPT-ENSO) and PDO (ANPP~PPT-PDO). Differences between ANPP~PPT PASC and the respective PASC after teleconnection effect removal are shown in red italics and parentheses.

Site	ANPP~PPT	ANPP~PPT-ENSO	ANPP~PPT-PDO
JRN	65	58 *(-7)*	57 *(-8)*
SEV	44	20 *(-24)*	15 *(-29)*
KNZ	53	32 *(-21)*	33 *(-20)*
SGS	32	20 *(-12)*	4 *(-28)*
CDR	20	15 *(-5)*	14 *(-6)*
KBS	47	30 *(-17)*	23 *(-24)*

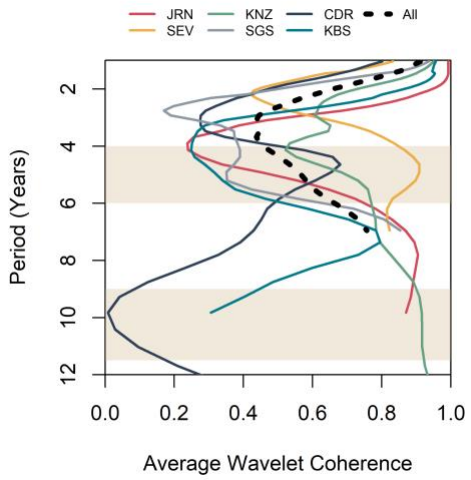

Figure 3. Average wavelet coherence across periods for each site and average across all sites. Only values outside of the cone of influence were averaged. Brown polygons designate the periods where ENSO and PDO have the highest power from their individual wavelet transforms.

Obj. 2: Across sites, PASC decreased after excluding the effects of PDO or ENSO. However, the magnitude of that effect varied greatly among sites, ranging from 5-24% for ENSO and 6-29% for PDO (Table 1). Excluding effects of PDO and ENSO had the largest influence on the coherence between PPT and ANPP for SEV, KNZ, SGS, and KBS, where PASC was reduced by 24-29%, 21-20%, 12-28%, and 17-24% respectively (Table 1). PDO had a slightly stronger impact than ENSO on most sites, and especially SGS (28% reduction from ANPP~PPT PASC of 32%, compared with a reduction of 12% removing ENSO). Studies at SEV (Collins et al. 2020) and SGS (Chen et al. 2017) have documented similar significant responses of ANPP to PDO and ENSO. Parsing out the period space (e.g. 1-2 years, 2-6, 6-13) may identify at what exact temporal scales these teleconnections have the most impact, how that changes regional patterns, and whether that makes sense dynamically (e.g. Hu et al. 2021, Zhu et al. 2022). For example, when only examining periods 2-13years, JRN, SEV and KNZ are the most influenced by ENSO and PDO (not shown). Differences in the time frame and length between sites may influence the measured impacts of PDO and ENSO, especially as ENSO and PDO phases can interact to influence precipitation and production (e.g. Chen et al. 2017).

These perceived ENSO and PDO effects on the PPT ANPP relationship may be conflated with other potential explanatory variables, such as temperature (all of these sites have experienced warming in recent decades (Hudson et al. 2022)), or the periodicity in plant species population and community dynamics. To separate these parts out, knowledge of site level dynamics of ANPP is required, and could potentially be included as additional variables in the partial wavelet coherence analysis. This may also allow us to further disentangle coherence differences within regions. JRN and SEV are located within the same region, however, when we truncate JRN to 1999-2018 to match SEV, there are major differences in wavelet coherence maps (not shown). This could be an indication of the spatially heterogeneous precipitation in the

region (e.g. the monsoonal system) and/or major differences in the production and community structures at these sites.

While this work indicates that multi-year precipitation periods are related to production response at most central US grasslands, sub-annual breakdowns of coherence would be interesting to explore in future studies. Wavelet analyses require data on the same time step. Only the desert grasslands collect biomass data sub-annually, so other methods and proxies for ANPP (e.g. satellite data or eddy covariance flux tower data; Chen et al. 2017) would need to be applied to compare all sites. The PDO and ENSO-driven mechanisms of precipitation delivery can be season dependent and so a sub-annual approach may also facilitate parsing out the relative effects of these teleconnections on ANPP PPT coherence.

Conclusions

We applied wavelet coherence analysis to over 20 years of annual precipitation and plant production data and found that the short (1-2 year) periods typically exhibited the strongest coherence across sites, however, coherence was not always consistent in strength. Sites in the south central U.S. also exhibited strong coherence at long (5-10 year) periods. This regional variability in period coherence is likely due in part to the semi-periodic climatological drivers of precipitation in a region, as well as the frequency and intensity of disturbance events grasslands are exposed to. PDO and ENSO impacted the coherence across multiple sites, indicating that there may be some ability to forecast ANPP given PPT projections and climate mode phases, although further work is needed to establish at what periods could provide the most predictive power. In a changing climate, with increasingly frequent and intense disturbance events, analyses able to incorporate non-stationary data to identify periods of strong coherence may improve models of grassland production.

Acknowledgements

Funding was provided by the USDA-ARS SCINet Big Data Project (grant no. 0500–00093–001–00-D). LTER site researchers (John Blair, Daniel Childers, Peter Doran, Michael Gooseff, Katherine Gross, Nick Haddad, Melissa Pastore, Jennifer Rudgers, Osvaldo Sala, Eric Seabloom, and Gaius Shaver) contributed to the selection and harmonization of representative, site-level precipitation and ANPP datasets used here and in Hudson et al. (2022).

References

Borchers, H.W. 2021. pracma: Practical Numerical Math Functions. R package version 2.3.6.

Cazelles, B., Chavez, M., Berteaux, D., Ménard, F., Vik, J. O., Jenouvrier, S., and Stenseth, N. C. 2008. Wavelet analysis of ecological time series. *Oecologia*, 156(2): 287–304.

Chen, M., Parton, W. J., DelGrosso, S. J., Hartman, M. D., Day, K. A., Tucker, C. J., et al. 2017. The signature of sea surface temperature anomalies on the dynamics of semiarid grassland productivity. *Ecosphere*, *8*(12).

Collins, S. L., Chung, Y. A., Baur, L. E., Hallmark, A., Ohlert, T. J., and Rudgers, J. A. 2020. Press–pulse interactions and long-term community dynamics in a Chihuahuan Desert grassland. *Journal of Vegetation Science*, 1–11.

Gouhier, T.C., Grinsted, A., Simko, V. 2021. R package biwavelet: Conduct Univariate and Bivariate Wavelet Analyses (Version 0.20.21).

Haddad N.M., Tilman D., and Knops J.M.H. 2002. Long-term oscillations in grassland productivity induced by drought. *Ecology Letters*, 5: 110-120.

Harrell, F. 2021. Hmisc: Harrell Miscellaneous. R package version 4.6-0.

Hobbie, J. E., Carpenter, S. R., Grimm, N. B., Gosz, J. R., & Seastedt, T. R. (2003). The US Long Term Ecological Research Program. *BioScience*, *53*(1), 21–32.

Hu, W., and Si, B. 2021. Technical Note : Improved partial wavelet coherency for understanding scale-specific and localized bivariate relationships in geosciences, 321–331.

Hudson, A.R., Peters, D.P.C., Blair, J.M., Childers, D.L., Doran, P.T., Geil, K., Gooseff, M., Gross, K.L., Haddad, N.M., Pastore, M.A., Rudgers, J.A., Sala, O., Seabloom, E.W., and Shaver, G. 2022. Cross-site comparisons of dryland ecosystem response to climate change in the US Long-Term Ecological Research network. *BioScience*, 72(9): 889-907.

Lauenroth, W. 2014. SGS-LTER Standard Production Data: 1983-2008 Annual Aboveground Net Primary Production on the Central Plains Experimental Range, Nunn, Colorado, USA 1983-2008, ARS Study Number 6 ver 1. Environmental Data Initiative. https://doi.org/10.6073/pasta/f9462ef45391dfa873e43383a179022d (Accessed 2022-10-19).

Lauenroth, W. K. and Burke, I. C. 1995. The Great Plains: Climate variability. Encyclopedia of environmental biology, Volume 2. Academic Press, Inc. 237-249.

Mantua, N., Hare, S., Zhang, Y., Wallace, J., Francis, R. 1997. A Pacific interdecadal climate oscillation with impacts on salmon production. *Bulletin of the American Meteorological Society*, 78: 1069-1079.

Olson, D. M., Dinerstein, E., Wikramanayake, E. D., Burgess, N. D., Powell, G. V. N., Underwood, E. C., D'Amico, J. A., Itoua, I., Strand, H. E., Morrison, J. C., Loucks, C. J., Allnutt, T. F., Ricketts, T. H., Kura, Y., Lamoreux, J. F., Wettengel, W. W., Hedao, P., Kassem, K. R. 2001. Terrestrial ecoregions of the world: a new map of life on Earth. *Bioscience* 51(11):933-938.

Parton, W. 2014. SGS-LTER Standard Met Data: Cr21x Station 12 - Daily Meteorological Data on the Central Plains Experimental Range in Nunn, Colorado, USA 1986-2010, ARS Study Number 4 ver 17. *Environmental Data Initiative*. https://doi.org/10.6073/pasta/fff09a9c72366784518bc875da91b03e (Accessed 2022-10-13).

Peters, D.P.C., Savoy, H.M., Stillman, S., Huang, H., Hudson, A.R., Sala, O.E., and Vivoni, E.R. 2021. Plant Species Richness in Multiyear Wet and Dry Periods in the Chihuahuan Desert. *Climate*, 9(8): 130.

Petrie, M. D., Peters, D. P. C., Yao, J., Blair, J. M., Burruss, N. D., Collins, S. L., Derner, J.D., Gherardi, L.A., Hendrickson, J.R., Sala, O.E., Starks, P.J., and Steiner, J.L. 2017. Regional grassland productivity responses to precipitation during multiyear above- and below-average rainfall periods. *Global Change Biology*, 24(5): 1935–1951.

Pohlert, T. 2020. Trend: Non-Parametric Trend Tests and Change-Point Detection. R package version 1.1.4.

R Core Team. 2021. R: A language and environment for statistical computing. R Foundation for Statistical Computing, Vienna, Austria. https://www.R-project.org/.

Rayner, N., Parker, D., Horton, E., Folland, C., Alexander, L., Rowell, D., Kent, E., Kaplan, A. 2003. Global analyses of sea surface temperature, sea ice, and night marine air temperature since the late nineteenth century. *J. Geophys. Res.*, 108 (D14): 4407.

Shoop, M., Wasser, C.H., Engel, A., Hazlett, D., Augustine, D., Martyn, T., Milchunas, D., Stapp, P., Kaplan, N., Lindquist, M. Working list of plants used by the SGS-LTER Program on the Central Plains Experimental Range, Nunn, Colorado. http://hdl.handle.net/10217/80451 (Accessed 2022-10-13).

Zhou, Z., Liu, S., Ding, Y., Fu, Q., Wang, Y., Cai, H., and Shi, H. 2022. Assessing the responses of vegetation to meteorological drought and its influencing factors with partial wavelet coherence analysis. *Journal of Environmental Management*, 311: 114879.